

Estimation of a Causal Directed Acyclic Graph Process using Non-Gaussianity

Aref Einizade and Sepideh Hajipour Sardouie

Abstract—Numerous approaches have been proposed to discover causal dependencies in machine learning and data mining; among them, the state-of-the-art VAR-LiNGAM (short for Vector Auto-Regressive Linear Non-Gaussian Acyclic Model) is a desirable approach to reveal *both* the instantaneous and time-lagged relationships. However, all the obtained VAR matrices need to be analyzed to infer the final causal graph, leading to a rise in the number of parameters. To address this issue, we propose the CGP-LiNGAM (short for Causal Graph Process-LiNGAM), which has significantly fewer model parameters and deals with only *one* causal graph for interpreting the causal relations by exploiting Graph Signal Processing (GSP).

Index Terms—Causal Discovery, Graph Signal Processing (GSP), Causal Graph Process (CGP), Linear Non-Gaussian Acyclic Model (LiNGAM), Directed Acyclic Graph (DAG).

I. INTRODUCTION

Causal Discovery (CD) [1], [2] of time-series data, also known as Dynamic CD (DCD), has gained significant attention due to its capability to reveal causal relationships between observational data. A wide variety of DCD methods have been proposed based on different points of view. For a comprehensive survey, please refer to [3] and the references therein. Two popular and well-known types of causal dependency order are instantaneous and time-lagged ones which are mostly addressed by Structural Equation Model (SEM) [2], and Vector Auto-Regressive (VAR) ones [2]. Among the SEM-based approaches, the popular Linear Non-Gaussian Acyclic Model (LiNGAM) addresses the identifiability issue by assuming the exogenous disturbances are non-Gaussian [4]. Besides, the state-of-the-art VAR-LiNGAM method [5] has been proposed to reveal both the instantaneous and time-lagged dependencies. As well as desirable advantages of the VAR and VAR-LiNGAM, having a high number of free model parameters and the need for interpreting all VAR matrix coefficients to infer the final causal graph are still major drawbacks [6].

On the other hand, in most recording systems of time-series, the interacting sensors, such as brain regions [7], geographic temperature locations [6], etc., can be considered the nodes of a meaningful underlying (and possibly directed) causal graph. For example, the learned graphs from brain signals can reveal the directed interactions between latent brain sources [5]. These graphs are rarely known in real machine learning applications and need to be carefully learned/estimated from observational data [3], [7]. Building upon this causal graph, the different recorded measurements on different nodes (in

one time index) can be interpreted as a graph signal, which provides utilizing Graph Signal Processing (GSP) tools [8], [9], [6], [10] in different areas such as image [11], [12], [13] and video [14], [15] processing.

Recently, a GSP-based method named Causal Graph Process (CGP) [6] has been proposed to address the mentioned drawbacks of the VAR by modeling the VAR coefficient matrices with graph polynomial filters; however, this model can not model the instantaneous dependencies. To address the mentioned issues, in the proposed (graph) shift invariant [6] CGP-LiNGAM analysis, the discovery of causal relationships relies on only *one* and *shared* underlying Directed Acyclic Graph (DAG) [6] to reveal both the instantaneous and time-lagged dependencies, unlike almost all of the other VAR-based approaches, such as VAR-LiNGAM [5] and DYNOTEARS [16], [17], [18], which need analyzing all the obtained VAR matrix coefficients to infer the underlying causal graph. The main contributions of the present paper are summarized as:

- The proposed CGP-LiNGAM reveal both the instantaneous and time-lagged dependencies, and, is related to only *one* and *shared* underlying Directed Acyclic Graph (DAG) [6] (significantly fewer parameters, based on the analysis presented in Section (III-D)) unlike the state-of-the-art VAR-LiNGAM [5] and DYNOTEARS [18].
- We present closed-form iteration-based solutions in Section III, which facilitate applicability and reproducibility.
- Non-Gaussianity of the exogenous disturbances guarantees the identifiability of the proposed model [5].
- Based on the experimental analysis in Sections IV-A, IV-B and IV-C, the CGP-LiNGAM performs more accurately and robust in causal graph recovery and prediction tasks compared to the VAR-LiNGAM [5], and DYNOTEARS [18].
- Based on the additional presented analysis in Section IV-D, the CGP-LiNGAM method is also robust in the case of not known CGP (VAR) order [19].

The notations $(\cdot)^T$, \otimes , $(\cdot)^\dagger$, $\|\cdot\|_p$, and \hat{x} stand for transpose operator, Kronecker product, Moore-Penrose pseudo-inverse of a matrix, the p -norm of a vector, and the estimation of the true entity x , respectively.

II. RELATED WORK AND BACKGROUND

The observation matrix $\mathbf{X} = (\mathbf{x}(0), \mathbf{x}(1), \dots, \mathbf{x}(K-1)) \in \mathbb{R}^{N \times K}$ is provided to us by recording K -length signals on N sensors/nodes. In the following, the related work/background is briefly reviewed as follows:

Aref Einizade, and Sepideh Hajipour Sardouie (Corresponding author, email: hajipour@sharif.edu) are with the Department of Electrical Engineering, Sharif University of Technology, Tehran, Iran.

LiNGAM. In an (instantaneous) SEM (1), assuming the exogenous disturbance \mathbf{e} is non-Gaussian, the underlying DAG \mathbf{A} can be uniquely recovered by the LiNGAM analysis [4]:

$$\mathbf{x}(k) = \mathbf{A}\mathbf{x}(k) + \mathbf{e}(k) \quad (1)$$

VAR. The VAR modeling of time-series \mathbf{X} is defined as:

$$\mathbf{x}(k) = \sum_{i=1}^M \mathbf{A}^{(i)} \mathbf{x}(k-i) + \mathbf{e}(k) \quad (2)$$

where M denotes the VAR-order, and $\{\mathbf{A}^{(i)}\}_{i=1}^M$ are VAR coefficient matrices [5]. From the Granger [20] analysis point of view, to recover the underlying causal graph \mathbf{A}' modeling the causal relationships, one considers $\mathbf{A}'_{ij} = 0$, if $\mathbf{A}^{(k)}_{ij} = 0$ for all k [21], [6], implying the conditional independence between the time-series at each node described by a Markov Random Field (MRF) with adjacency structure \mathbf{A}' [6].

VAR-LiNGAM. In this method, both the instantaneous and time-lagged dependencies are modeled using the combination of (1) and (2) as [5]:

$$\mathbf{x}(k) = \sum_{i=0}^M \mathbf{A}^{(i)} \mathbf{x}(k-i) + \mathbf{e}(k) \quad (3)$$

In this method, $\mathbf{A}^{(0)}$ is considered a DAG, and the exogenous disturbance \mathbf{e} is assumed to be non-Gaussian to guarantee the identifiability [5]. Then, similar to the VAR model (2), the sparsity pattern of all $\{\mathbf{A}^{(i)}\}_{i=0}^M$ must be analysed to recover the true underlying causal graph \mathbf{A}' [5].

GSP background. A (possibly directed) graph $\mathcal{G} = (\mathbf{V}, \mathbf{A})$ is characterized by its vertex set $\mathbf{V} = \{v_1, \dots, v_N\}$ and its adjacency matrix $\mathbf{A} \in \mathbb{R}^{N \times N}$. If $\mathbf{A}_{ij} \neq 0$, the i th node is a parent of the j th node, and the j th node is a descendant of the i th node [2]. We call a node *pure parent*, if it is not the descendant of any other nodes. A graph signal $\mathbf{x} = (x_1, \dots, x_N)^T \in \mathbb{R}^{N \times 1}$ is a mapping $\mathbf{x} : \mathbf{V} \rightarrow \mathbb{R}$, assigning the i th vertex the value of x_i [8]. A L -order graph polynomial filter is also defined as $c(\mathbf{A}) = c_0 \mathbf{I} + c_1 \mathbf{A} + \dots + c_L \mathbf{A}^L$ [6], where \mathbf{I} denotes the identity matrix of size N .

Causal Graph Process (CGP). An M -order CGP model has the following form [6]:

$$\mathbf{x}(k) = \sum_{i=1}^M P_i(\mathbf{A}, \mathbf{c}) \mathbf{x}(k-i) + \mathbf{e}(k) \quad (4)$$

where $P_i(\mathbf{A}, \mathbf{c}) = \sum_{j=0}^i c_{ij} \mathbf{A}^j$ and \mathbf{c} collects the scalar polynomial coefficients as $(1 \leq i \leq M \text{ and } 0 \leq j \leq i)$:

$$\mathbf{c} = (c_{10}, c_{11}, \dots, c_{ij}, \dots, c_{MM})^T \quad (5)$$

III. THE PROPOSED CGP-LiNGAM APPROACH

In our CGP-LiNGAM framework, the instantaneous (LiNGAM) and time-lagged (CGP) parts share *one* underlying DAG \mathbf{A} . To recover both these causal dependencies, our (graph) shift invariant [22] proposed framework is shown as:

$$\mathbf{x}(k) = \mathbf{A}\mathbf{x}(k) + \sum_{i=1}^M \overbrace{P_i(\mathbf{A}, \mathbf{c})}^{\mathbf{R}_i} \mathbf{x}(k-i) + \mathbf{e}(k) \quad (6)$$

The proposed model (6) can be rewritten as:

$$\mathbf{x}(k) = \sum_{i=1}^M \tilde{\mathbf{R}}_i \mathbf{x}(k-i) + \tilde{\mathbf{e}}(k) \quad (7)$$

where the following theorem helps to recover $\tilde{\mathbf{R}}_i$ in (7), and

$$\tilde{\mathbf{R}}_i = (\mathbf{I} - \mathbf{A})^{-1} \mathbf{R}_i; \quad \tilde{\mathbf{e}}(k) = (\mathbf{I} - \mathbf{A})^{-1} \mathbf{e}(k) \quad (8)$$

Theorem 1: In the model (7), $\tilde{\mathbf{R}}_i$ and $\tilde{\mathbf{R}}_j$ commute, i.e., $\tilde{\mathbf{R}}_i \tilde{\mathbf{R}}_j = \tilde{\mathbf{R}}_j \tilde{\mathbf{R}}_i$, for $i, j = 1, 2, \dots, N$ under the conditions:

A1) \mathbf{A} is a DAG.

A2) $\forall i : |\lambda_i(\mathbf{A})| < 1$, where $\lambda_i(\mathbf{A})$ is the i th eigenvalue of \mathbf{A} .

Proof: If \mathbf{A} is a DAG, $\mathbf{I} - \mathbf{A}$ is invertible [4], [5], and if $\forall i : |\lambda_i(\mathbf{A})| < 1$, the the infinite sum of the geometric series $\sum_{r=0}^{\infty} \mathbf{A}^r$ is summable, and equal to $(\mathbf{I} - \mathbf{A})^{-1}$ as [23]:

$$(\mathbf{I} - \mathbf{A})^{-1} = \sum_{r=0}^{\infty} \mathbf{A}^r \quad (9)$$

Then, the VAR coefficient matrices $\{\tilde{\mathbf{R}}_i\}_{i=1}^M$ in (7) commute because they can be as (infinite) graph polynomial filters:

$$\begin{aligned} \tilde{\mathbf{R}}_i &= (\mathbf{I} - \mathbf{A})^{-1} \mathbf{R}_i = \left[\sum_{r=0}^{\infty} \mathbf{A}^r \right] \left[\sum_{j=0}^i c_{ij} \mathbf{A}^j \right] \\ &= \sum_{r=0}^{\infty} \sum_{j=0}^i c_{ij} \mathbf{A}^{r+j}. \quad \blacksquare \end{aligned} \quad (10)$$

In the following, the proposed three-step approach for recovering $\{\tilde{\mathbf{R}}_i\}_{i=1}^M$, \mathbf{A} , $\{\mathbf{R}_i\}_{i=1}^M$, and \mathbf{c} is presented.

A. Recovering $\{\tilde{\mathbf{R}}_i\}_{i=1}^M$

Based on Theorem 1, the commutativity terms are included in the following multi-convex optimization [6] to obtain the (possibly sparse) graph polynomial filters $\{\tilde{\mathbf{R}}_i\}_{i=1}^M$ as:

$$\begin{aligned} \hat{\tilde{\mathbf{R}}}_i &= \underset{\tilde{\mathbf{R}}_i}{\operatorname{argmin}} \frac{1}{2} \sum_{k=M}^{K-1} \left\| \mathbf{x}(k) - \sum_{i=1}^M \tilde{\mathbf{R}}_i \mathbf{x}(k-i) \right\|_2^2 + \lambda_1 \|\operatorname{vec}(\tilde{\mathbf{R}}_1)\|_1 \\ \text{Subject to: } & \tilde{\mathbf{R}}_i \tilde{\mathbf{R}}_j = \tilde{\mathbf{R}}_j \tilde{\mathbf{R}}_i; \quad i, j = 1, \dots, N \end{aligned} \quad (11)$$

An alternating optimization to (11) is expressed as:

$$\begin{aligned} \hat{\tilde{\mathbf{R}}}_i &= \underset{\tilde{\mathbf{R}}_i}{\operatorname{argmin}} \frac{1}{2} \sum_{k=M}^{K-1} \left\| \mathbf{x}(k) - \sum_{i=1}^M \tilde{\mathbf{R}}_i \mathbf{x}(k-i) \right\|_2^2 \\ &+ \lambda_1 \|\operatorname{vec}(\tilde{\mathbf{R}}_1)\|_1 + \lambda_3 \sum_{i \neq j} \|\tilde{\mathbf{R}}_i \tilde{\mathbf{R}}_j - \tilde{\mathbf{R}}_j \tilde{\mathbf{R}}_i\|_F^2 \end{aligned} \quad (12)$$

where, with the definitions $\mathbf{X}_m = (\mathbf{x}(m), \mathbf{x}(m+1), \dots, \mathbf{x}(m+K-M-1))$ and $\tilde{\mathbf{r}}_i = \operatorname{vec}(\tilde{\mathbf{R}}_i)$, (12) can be rewritten as (with the details [24] in the Appendix section):

$$\hat{\tilde{\mathbf{r}}}_i = \underset{\tilde{\mathbf{r}}_i}{\operatorname{argmin}} \|\Psi_i \tilde{\mathbf{r}}_i - \tilde{\mathbf{y}}_i\|_2^2 + \lambda_1 \|\tilde{\mathbf{r}}_1\|_1 \quad (13)$$

where $\mathbf{0}$ is a all-zero array with appropriate size, and

$\Psi_i =$

$$\left(\frac{\sqrt{2}}{2} \mathbf{B}_i^T, \sqrt{\lambda_3} \Phi_1^T, \dots, \sqrt{\lambda_3} \Phi_{i-1}^T, \sqrt{\lambda_3} \Phi_{i+1}^T, \dots, \sqrt{\lambda_3} \Phi_M^T \right)^T \quad (14)$$

$$\tilde{\mathbf{y}}_i = \left(\frac{\sqrt{2}}{2} \mathbf{y}_i^T, \mathbf{0}^T, \dots, \mathbf{0}^T \right)^T \quad (15)$$

$$\begin{aligned} \mathbf{B}_i &= \mathbf{X}_{M-i}^T \otimes \mathbf{I}, \quad \Phi_i = \mathbf{R}_i^T \otimes \mathbf{I} - \mathbf{I}^T \otimes \mathbf{R}_i, \\ \mathbf{y}_i &= \text{vec}(\mathbf{X}_M) - \text{vec} \left(\sum_{j=1 \neq i}^M \tilde{\mathbf{R}}_j \mathbf{X}_{M-j} \right) \end{aligned} \quad (16)$$

Afterwards, the *unique* (identifiable) [6] closed-form solutions to (12) are expressed as:

$$\hat{\mathbf{r}}_{i \neq 1} = \Psi_i^\dagger \tilde{\mathbf{y}}_i, \quad i = 2, \dots, M \quad (17)$$

and $\hat{\mathbf{r}}_1$ can be obtained using standard l_1 minimization approaches in (13), such as LASSO [25].

B. Recovering \mathbf{A}

By recovering $\{\tilde{\mathbf{R}}_i\}_{i=1}^M$, the residual $\tilde{\mathbf{e}}$ is also obtained from (7), and the relation $\tilde{\mathbf{e}}(k) = (\mathbf{I} - \mathbf{A})^{-1} \mathbf{e}(k)$ can be rewritten:

$$\tilde{\mathbf{e}}(k) = \mathbf{A} \tilde{\mathbf{e}}(k) + \mathbf{e}(k) \quad (18)$$

which is an SEM, and, due to the non-Gaussianity of the exogenous disturbance \mathbf{e} , the underlying DAG \mathbf{A} can be *uniquely* (identifiable) inferred using the LiNGAM analysis [4], [5] on $\tilde{\mathbf{e}}$ exploiting FastICA [26] approach.

C. Recovering $\{\mathbf{R}_i\}_{i=1}^M$ and \mathbf{c}

By recovering $\{\tilde{\mathbf{R}}_i\}_{i=1}^M$ and \mathbf{A} , the graph polynomial filters $\{\mathbf{R}_i = (\mathbf{I} - \mathbf{A})\tilde{\mathbf{R}}_i\}_{i=1}^M$ are obtained, and, inspiring from the CGP model [6] (i.e., $\mathbf{R}_i = P_i(\mathbf{A}, \mathbf{c}) = \sum_{j=0}^i c_{ij} \mathbf{A}^j$), the polynomial coefficients \mathbf{c} are estimated by minimizing the following convex optimization using standard l_1 -regularized least squares methods, such as LASSO [25]:

$$\hat{\mathbf{c}}_i = \underset{\mathbf{c}_i}{\operatorname{argmin}} \frac{1}{2} \left\| \text{vec}(\hat{\mathbf{R}}_i) - \mathbf{Q}_i \mathbf{c}_i \right\|_2^2 + \lambda_2 \|\mathbf{c}_i\|_1 \quad (19)$$

where $\mathbf{Q}_i = \left(\text{vec}(\mathbf{I}), \text{vec}(\hat{\mathbf{A}}), \dots, \text{vec}(\hat{\mathbf{A}}^i) \right)$, and $\mathbf{c}_i = (c_{i0}, c_{i1}, \dots, c_{ii})^T$ [6] for $i = 1, \dots, M$. Concisely, our proposed CGP-LiNGAM algorithm is summarized in Algorithm 1.

D. Number of learnable model parameters

In the CGP-LiNGAM (6), the underlying DAG \mathbf{A} has $\frac{N(N-1)}{2}$ free parameters (because of the technically being lower triangular), and $\mathbf{c} \in \mathbb{R}^{\frac{M(M+3)}{2}}$, compared to the VAR-LiNGAM [5] (3), which needs $\frac{N(N-1)}{2} + MN^2$ free parameters to describe the model. On the other hand, in real application, usually $N \gg M$ [5], [6], so the CGP-LiNGAM (with combined $\frac{N(N-1)}{2} + \frac{M(M+3)}{2}$ free parameters) is considerably parsimonious compared to the VAR-LiNGAM.

Algorithm 1 : CGP-LiNGAM

Input: $\mathbf{X} \in \mathbb{R}^{N \times T}$, M , $\{\lambda_i\}_{i=1}^3$
Output: Causal DAG $\mathbf{A} \in \mathbb{R}^{N \times N}$, Polynomial coefficients \mathbf{c}

- 1: Initialize: $t = 1$, $\hat{\mathbf{R}}^{(0)} = \mathbf{0}$
- 2: **while** Convergence **do**
- 3: **for** $i = 1 : M$ **do**
- 4: Estimate $\tilde{\mathbf{R}}_i^{(t)}$ by fixing $\{\tilde{\mathbf{R}}_j^{(t-1)}\}_{j=1 \neq i}^M$, and using CVX [27] in (11) or (12), or using LASSO[25]/closed-form solutions in (17)
- 5: **end for**
- 6: $t \leftarrow t + 1$
- 7: **end while:** return $\{\tilde{\mathbf{R}}_i\}_{i=1}^M$ and $\tilde{\mathbf{e}}$ in (7)
- 8: Estimate $\mathbf{R}_0 = \mathbf{A}$ using LiNGAM analysis [4] on $\tilde{\mathbf{e}}$
- 9: Obtain the causal effect matrices $\{\mathbf{R}_i = (\mathbf{I} - \mathbf{A})\tilde{\mathbf{R}}_i\}_{i=1}^M$
- 10: Solve for \mathbf{c} in (19) by l_1 minimization, e.g., LASSO [25]

E. Complexity Analysis of CGP-LiNGAM (Algorithm 1)

For a specific i and an convergence iteration in Line 4, optimization (12) is naively dominated by the matrix-matrix product of $\{\tilde{\mathbf{R}}_i \tilde{\mathbf{R}}_j\}_{j=1 \neq i}^M$ with $\mathcal{O}((M-1)N^3)$, and matrix-vector product of $\{\mathbf{R}_j \mathbf{x}(k-j)\}_{k=M, j=1}^{K-1, M}$ with $\mathcal{O}((K-M)N^2)$ complexity [6]. As a result, the overall complexity of one convergence iteration is $\mathcal{O}(M^2N^3 + KMN^2)$. In Line 8, the computational complexity of the LiNGAM analysis typically $\mathcal{O}(KN^3 + N^4)$ [28]. The matrix-matrix products of $\{(\mathbf{I} - \mathbf{A})\tilde{\mathbf{R}}_i\}_{i=1}^M$ in Line 9 take total complexity of $\mathcal{O}(MN^3)$. In Line 10, the minimization (19) for each i is dominated by multiplications $\mathbf{Q}_i^T \mathbf{Q}_i \in \mathbb{R}^{(i+1) \times (i+1)}$ and $\mathbf{Q}_i^T \text{vec}(\tilde{\mathbf{R}}_i) \in \mathbb{R}^{(i+1) \times 1}$, which take $\mathcal{O}((i+1)^2)$ operations [6], and, combined complexity of $\mathcal{O}(M(\sum_{i=1}^M (i+1)^2)) \approx \mathcal{O}(M^4)$. All in all, assuming $M \ll K$, the total (worst-case and naive) computational complexity of Algorithm 1 is approximately $\mathcal{O}(KMN^2 + KN^3 + N^4 + M^4)$. Note that the (possible) sparsity of the underlying DAG can severely reduce the complexity [6].

IV. EXPERIMENTAL RESULTS AND DISCUSSION

In this section, we provide experimental analysis in two categories: 1) ablation study: analyzing the performance of the CGP-LiNGAM in different situations, 2) comparison study: comparing the performance of the CGP-LiNGAM with that of the state-of-the-art, i.e., VAR-LiNGAM [5]. The underlying DAG \mathbf{A} and also the non-Gaussian exogenous disturbance \mathbf{e} are generated as described in [4]. Note that, to have sparse DAGs, we generate \mathbf{A} (with $N = 5$) with just *one* pure parent. The generated data were divided into three parts of the train, validation (to find the optimal hyperparameters using grid search) and test (to evaluate the prediction based on the optimized model) [6].

A. Ablation Study

We vary the number of samples K and the CGP-order M in the spans of $\{300, 500, 700, 900\}$ and $\{2, 5, 7, 10\}$, respectively, to study the effect of these changes on the recovery performance. The polynomial coefficients \mathbf{c} are

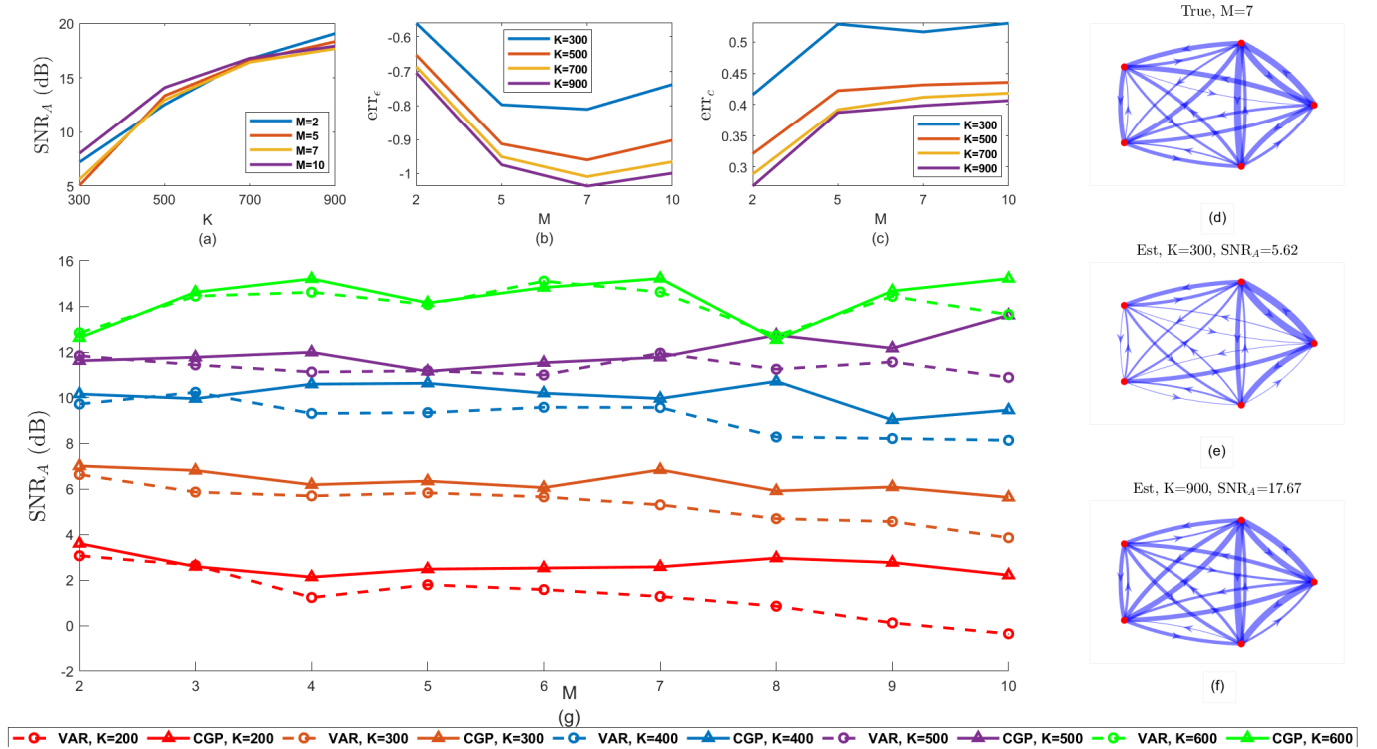


Fig. 1. (a-c) The average of the performance evaluation metrics over thirty Monte-Carlo realizations, by varying the number of samples K and the CGP-order M in the spans of $\{300, 500, 700, 900\}$ and $\{2, 5, 7, 10\}$, respectively. (d-f): An example average ($M = 7$) to the graph structures (Figure 1, (d:f)) over Monte-Carlo realizations. (g): Comparison of the graph recovery performance of the proposed CGP-LiNGAM method with the celebrated VAR-LiNGAM [5]

generated as $2^{i+j}c_{ij} \sim 0.5[\mathcal{U}(-1, -0.45) + \mathcal{U}(0.45, 1)]$ to model coefficient decay with distance to the current time sample [6]. Besides, to evaluate the quality of the recoveries, we consider the following scale-free metrics $SNR_A = 20 \log(\|\mathbf{A}\|_F / \|\hat{\mathbf{A}} - \mathbf{A}\|_F)$, $err_\epsilon = \|\hat{\mathbf{c}} - \mathbf{c}\|_2 / \|\mathbf{c}\|_2$, and

$$err_\epsilon = \mathbb{E} \left[\frac{1}{N} \|\mathbf{x}(k) - f(\hat{\mathbf{A}}, \hat{\mathbf{c}}, \mathbf{X}'_{k-1})\|_2^2 \right] - \mathbb{E} \left[\frac{1}{N} \|\mathbf{x}(k) - f(\mathbf{A}, \mathbf{c}, \mathbf{X}'_{k-1})\|_2^2 \right] \quad (20)$$

where $f(\mathbf{A}, \mathbf{c}, \mathbf{X}'_{k-1}) = \mathbf{A}\mathbf{x}(k) + \sum_{i=1}^M P_i(\mathbf{A}, \mathbf{c})\mathbf{x}(k-i)$, and err_ϵ models the prediction error on the test data [6]. Also, the expectations $\mathbb{E}\{\cdot\}$ in (20) are approximated by the sample mean over time samples. The average of the mentioned metrics and also an example average ($M = 7$) to the graph structures over thirty Monte-Carlo realizations are illustrated in Figure 1 (a:c), and (d:f), respectively. Note that although the underlying true graphs are acyclic, the plotted averaged ones can have cycles. From these results, it can be admitted that, on average, the graph recovery is superior in small values of M , i.e., $M = 2$, in case of having enough time samples, i.e., $K = 900$. Besides, the higher the number of the time samples K , the lower the prediction error err_ϵ [6]. Also, the err_ϵ is small and robust against the changes of M if the number of time samples is not very small, i.e., $K > 300$.

B. Comparison with State-of-the-art

In this subsection, we compare the graph recovery performance of the CGP-LiNGAM with the celebrated VAR-LiNGAM in Figure 1 (g) by varying K and M in the spans of $\{200 : 600\}$ and $\{2 : 9\}$, respectively. The polynomial coefficients \mathbf{c} are generated as $2^{i+j}c_{ij} \sim \mathcal{N}(1, 0.01)$. It is well illustrated in this figure that the CGP-LiNGAM is more robust and also superior compared to the VAR-LiNGAM, especially in a small number of time samples K , i.e., $K \leq 500$, and also in high values of causal dependency M , i.e., $M \geq 5$.

C. Comparison with DYNOTEARS [18]

The graph recovery results of the CGP-LiNGAM and DYNOTEARS [18] methods in different CGP order $M \in \{2, 5, 7\}$ and across time samples $K \in \{500, 1000, 2000, 5000\}$ are shown in Figure 2. It can be seen that a similar trend of improving the graph recovery with increasing the sample size K is observed in this figure for both methods; however, the DYNOTEARS [18] has clearly failed to successfully recover the true DAGs, while the CGP-LiNGAM has estimated them with high quality. The DYNOTEARS model can be stated as [18]:

$$\mathbf{x}(k) = \mathbf{A}\mathbf{x}(k) + \sum_{i=1}^M \mathbf{W}_i \mathbf{x}(k-i) + \mathbf{e}(k) \quad (21)$$

where *only* \mathbf{A} has been assumed to be an acyclic graph, and $\{\mathbf{W}_i\}_{i=1}^M$ are unconstrained coefficient matrices (like VAR-LiNGAM [5]) leading to increased number of learnable parameters to $\frac{N(N-1)}{2} + MN^2$, in comparison to the proposed

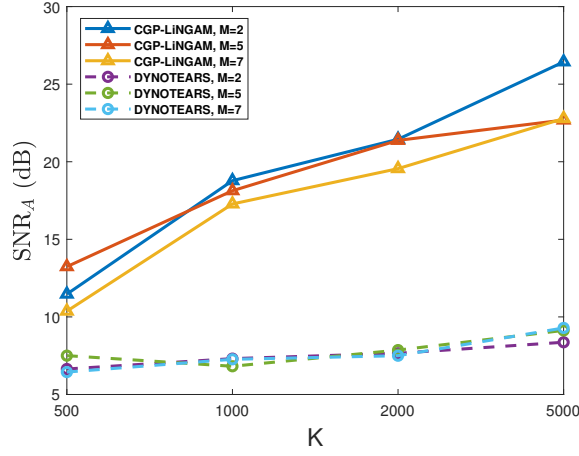


Fig. 2. Comparison of the graph recovery performance with the DYNOTEARS [18] method.

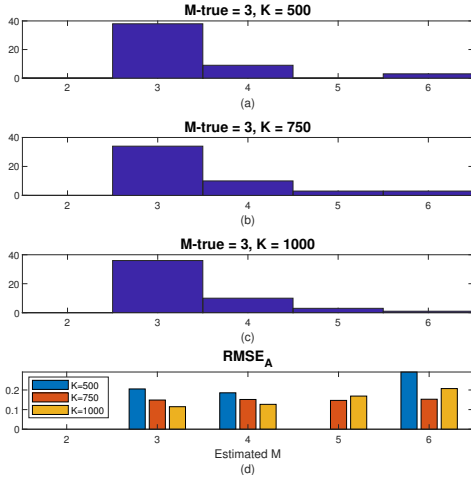


Fig. 3. (a)-(c): The histograms of the estimated M , in each $K \in \{500, 750, 1000\}$ based on minimum nAIC (22), (d): The averaged $\text{RMSE}_A = \frac{\|\hat{\mathbf{A}} - \mathbf{A}\|_F}{\|\mathbf{A}\|_F}$ over realizations of each selected M .

method which has significantly reduced $\frac{N(N-1)}{2} + \frac{M(M+3)}{2}$ learnable ones, because often $M \ll N$ [5], [6].

D. Choosing optimal CGP-order M

In most real applications, the CGP/VAR-order M is considered a fix or a prior known [6], [5], however, due to some uncertainty conditions, e.g., existing high amount of noise, choosing it optimally can considerably boost the recovery/modeling performance [19]. In this way, to investigate the possibility of correct selection of M , we generate fifty Monte-Carlo realizations similar to Section IV-B with CGP-order $M_{true} = 3$ and number of time samples $K \in \{500, 750, 1000\}$. Then, in each K , the normalized Akaike's Information Criterion (nAIC) (22) [19] is calculated in the span of $M \in \{2 : 6\}$ and the CGP-order M leading to minimum nAIC is considered as the estimation of M_{true} .

$$nAIC_{\hat{M}} = \log \left(\det \left(\frac{1}{K} \sum_{k=1}^K \hat{\mathbf{e}}(k) \hat{\mathbf{e}}(k)^T \right) \right) + \frac{2n_p}{K} \quad (22)$$

where $\det(\cdot)$ denotes the determinant operation, $\hat{\mathbf{e}}$ is the estimated disturbances corresponding to \hat{M} and the number of the estimated parameters $n_p = \frac{N(N-1)}{2} + \frac{\hat{M}(\hat{M}+3)}{2}$. Figure 3 (a)-(c) show the histograms of the estimated M , in each K . These results show that, in almost every K , M_{true} is successfully recovered. Moreover, in Figure 3 (d), the averaged $\text{RMSE}_A = \frac{\|\hat{\mathbf{A}} - \mathbf{A}\|_F}{\|\mathbf{A}\|_F}$ over realizations of each selected M is plotted, which shows that, even in selected wrong M cases, i.e., $M \neq M_{opt}$, the graph recovery remains fairly robust.

V. CONCLUSION

In this paper, we proposed the CGP-LiNGAM method to reveal both the instantaneous and time-lagged causal relationships in time-series by considering the node-specific time samples as graph signals on underlying causal DAGs. Compared to the state-of-the-art VAR-LiNGAM, our method has significantly fewer parameters, deals with only *one* underlying causal graph, and performs more robust against a low number of time samples and a high degree of causal dependency. Extending the CGP-LiNGAM to the time-varying graphs [29], [30] is our future research direction.

VI. APPENDIX (SIMPLIFICATIONS OF EQ. (12))

Due to the convexity of (12) w.r.t $\tilde{\mathbf{R}}_i$ (by fixing $\{\tilde{\mathbf{R}}_{j \neq i}\}_{j=1}^M$) [6], and with the definitions $\mathbf{X}_m = (\mathbf{x}(m), \mathbf{x}(m+1), \dots, \mathbf{x}(m+K-M-1))$ and $\tilde{\mathbf{r}}_i = \text{vec}(\tilde{\mathbf{R}}_i)$, the closed-form solutions can be obtained as:

$$\begin{aligned} \hat{\tilde{\mathbf{R}}}_i &= \underset{\tilde{\mathbf{R}}_i}{\text{argmin}} \frac{1}{2} \left\| \mathbf{X}_M - \sum_{j=1}^M \tilde{\mathbf{R}}_j \mathbf{X}_{M-j} \right\|_F^2 + \lambda_1 \|\text{vec}(\tilde{\mathbf{R}}_1)\|_1 \\ &+ \lambda_3 \sum_{j \neq i} \left\| [\tilde{\mathbf{R}}_i, \tilde{\mathbf{R}}_j] \right\|_F^2 \\ &= \underset{\tilde{\mathbf{R}}_i}{\text{argmin}} \frac{1}{2} \left\| \text{vec}(\tilde{\mathbf{R}}_i \mathbf{X}_{M-i}) - \overbrace{\text{vec} \left(\mathbf{X}_M - \sum_{j=1 \neq i}^M \tilde{\mathbf{R}}_j \mathbf{X}_{M-j} \right)}^{\mathbf{y}_i} \right\|_2^2 \\ &+ \lambda_1 \|\text{vec}(\tilde{\mathbf{R}}_1)\|_1 + \lambda_3 \sum_{j \neq i} \left\| \text{vec}(\tilde{\mathbf{R}}_i \tilde{\mathbf{R}}_j) - \text{vec}(\tilde{\mathbf{R}}_j \tilde{\mathbf{R}}_i) \right\|_2^2 \end{aligned} \quad (23)$$

Then, using the relation $\text{vec}(ABC) = (C^T \otimes A)\text{vec}(B)$ [24]:

$$\begin{aligned} \hat{\tilde{\mathbf{r}}}_i &= \underset{\tilde{\mathbf{r}}_i}{\text{argmin}} \frac{1}{2} \left\| \overbrace{(\mathbf{X}_{M-i}^T \otimes \mathbf{I}) \tilde{\mathbf{r}}_i - \mathbf{y}_i}^{\mathbf{B}_i} \right\|_2^2 + \lambda_1 \|\tilde{\mathbf{r}}_1\|_1 \\ &+ \lambda_3 \sum_{j \neq i} \left\| \overbrace{(\tilde{\mathbf{R}}_j^T \otimes \mathbf{I} - \mathbf{I}^T \otimes \tilde{\mathbf{R}}_j) \tilde{\mathbf{r}}_i}^{\Phi_j} \right\|_2^2 \\ &= \underset{\tilde{\mathbf{r}}_i}{\text{argmin}} \left\| \tilde{\Psi}_i \tilde{\mathbf{r}}_i - \tilde{\mathbf{y}}_i \right\|_2^2 + \lambda_1 \|\tilde{\mathbf{r}}_1\|_1 \end{aligned} \quad (24)$$

REFERENCES

- [1] Judea Pearl. *Causality*. Cambridge university press, 2009.
- [2] Jonas Peters, Dominik Janzing, and Bernhard Schölkopf. *Elements of causal inference: foundations and learning algorithms*. The MIT Press, 2017.
- [3] Charles K Assaad, Emilie Devijver, and Eric Gaussier. Survey and evaluation of causal discovery methods for time series. *Journal of Artificial Intelligence Research*, 73:767–819, 2022.
- [4] Shohei Shimizu, Patrik O Hoyer, Aapo Hyvärinen, Antti Kerminen, and Michael Jordan. A linear non-gaussian acyclic model for causal discovery. *Journal of Machine Learning Research*, 7(10), 2006.
- [5] Aapo Hyvärinen, Kun Zhang, Shohei Shimizu, and Patrik O Hoyer. Estimation of a structural vector autoregression model using non-gaussianity. *Journal of Machine Learning Research*, 11(5), 2010.
- [6] Jonathan Mei and José MF Moura. Signal processing on graphs: Causal modeling of unstructured data. *IEEE Transactions on Signal Processing*, 65(8):2077–2092, 2016.
- [7] Junzhong Ji, Aixiao Zou, Jinduo Liu, Cuicui Yang, Xiaodan Zhang, and Yongduan Song. A survey on brain effective connectivity network learning. *IEEE Transactions on Neural Networks and Learning Systems*, 2021.
- [8] Antonio Ortega, Pascal Frossard, Jelena Kovačević, José MF Moura, and Pierre Vandergheynst. Graph signal processing: Overview, challenges, and applications. *Proceedings of the IEEE*, 106(5):808–828, 2018.
- [9] Xiaowen Dong, Dorina Thanou, Laura Toni, Michael Bronstein, and Pascal Frossard. Graph signal processing for machine learning: A review and new perspectives. *IEEE Signal processing magazine*, 37(6):117–127, 2020.
- [10] Antonio Ortega. *Introduction to graph signal processing*. Cambridge University Press, 2022.
- [11] Xianming Liu, Gene Cheung, Xiangyang Ji, Debin Zhao, and Wen Gao. Graph-based joint dequantization and contrast enhancement of poorly lit jpeg images. *IEEE Transactions on Image Processing*, 28(3):1205–1219, 2018.
- [12] Gene Cheung, Enrico Magli, Yuichi Tanaka, and Michael K Ng. Graph spectral image processing. *Proceedings of the IEEE*, 106(5):907–930, 2018.
- [13] Chenggang Yan, Zhisheng Li, Yongbing Zhang, Yutao Liu, Xiangyang Ji, and Yongdong Zhang. Depth image denoising using nuclear norm and learning graph model. *ACM Transactions on Multimedia Computing, Communications, and Applications (TOMM)*, 16(4):1–17, 2020.
- [14] Anindya Mondal, Jhony H Giraldo, Thierry Bouwmans, Ananda S Chowdhury, et al. Moving object detection for event-based vision using graph spectral clustering. In *Proceedings of the IEEE/CVF International Conference on Computer Vision*, pages 876–884, 2021.
- [15] Jhony H Giraldo, Sajid Javed, Maryam Sultana, Soon Ki Jung, and Thierry Bouwmans. The emerging field of graph signal processing for moving object segmentation. In *International Workshop on Frontiers of Computer Vision*, pages 31–45. Springer, 2021.
- [16] Xun Zheng, Bryon Aragam, Pradeep K Ravikumar, and Eric P Xing. Dags with no tears: Continuous optimization for structure learning. *Advances in Neural Information Processing Systems*, 31, 2018.
- [17] Xun Zheng, Chen Dan, Bryon Aragam, Pradeep Ravikumar, and Eric Xing. Learning sparse nonparametric dags. In *International Conference on Artificial Intelligence and Statistics*, pages 3414–3425. PMLR, 2020.
- [18] Roxana Pamfil, Nisara Sriwattanaworachai, Shaan Desai, Philip Pilgerstorfer, Konstantinos Georgatzis, Paul Beaumont, and Bryon Aragam. Dynotears: Structure learning from time-series data. In *International Conference on Artificial Intelligence and Statistics*, pages 1595–1605. PMLR, 2020.
- [19] Lennart Ljung. System identification. In *Signal analysis and prediction*, pages 163–173. Springer, 1998.
- [20] Clive WJ Granger. Investigating causal relations by econometric models and cross-spectral methods. *Econometrica: journal of the Econometric Society*, pages 424–438, 1969.
- [21] Andrew Bolstad, Barry D Van Veen, and Robert Nowak. Causal network inference via group sparse regularization. *IEEE transactions on signal processing*, 59(6):2628–2641, 2011.
- [22] Antonio G Marques, Santiago Segarra, Geert Leus, and Alejandro Ribeiro. Stationary graph processes and spectral estimation. *IEEE Transactions on Signal Processing*, 65(22):5911–5926, 2017.
- [23] Ferenc Szidarovszky et al. *Introduction to Matrix Theory: with applications to business and economics*. World Scientific, 2002.
- [24] Kaare Brandt Petersen, Michael Syskind Pedersen, et al. The matrix cookbook. *Technical University of Denmark*, 7(15):510, 2008.
- [25] Robert Tibshirani. Regression shrinkage and selection via the lasso. *Journal of the Royal Statistical Society: Series B (Methodological)*, 58(1):267–288, 1996.
- [26] Aapo Hyvarinen. Fast and robust fixed-point algorithms for independent component analysis. *IEEE transactions on Neural Networks*, 10(3):626–634, 1999.
- [27] Michael Grant, Stephen Boyd, and Yinyu Ye. Cvx: Matlab software for disciplined convex programming, 2008.
- [28] Shohei Shimizu, Takanori Inazumi, Yasuhiro Sogawa, Aapo Hyvärinen, Yoshinobu Kawahara, Takashi Washio, Patrik O Hoyer, and Kenneth Bollen. Directlingam: A direct method for learning a linear non-gaussian structural equation model. *The Journal of Machine Learning Research*, 12:1225–1248, 2011.
- [29] Vassilis Kalofolias, Andreas Loukas, Dorina Thanou, and Pascal Frossard. Learning time varying graphs. In *2017 IEEE International Conference on Acoustics, Speech and Signal Processing (ICASSP)*, pages 2826–2830. Ieee, 2017.
- [30] Jhony H Giraldo, Arif Mahmood, Belmar Garcia-Garcia, Dorina Thanou, and Thierry Bouwmans. Reconstruction of time-varying graph signals via sobolev smoothness. *IEEE Transactions on Signal and Information Processing over Networks*, 8:201–214, 2022.